Environmetrics Special Issue Paper

Received: 12 July 2014, Revised: 10 November 2014, Accepted: 11 November 2014, Published online in Wiley Online Library: 16 December 2014

(wileyonlinelibrary.com) DOI: 10.1002/env.2324

Modeling individual tree growth by fusing diameter tape and increment core data

Erin M. Schliep[a*], Tracy Qi Dong[b], Alan E. Gelfand[a] and Fan Li[a]

Tree growth estimation is a challenging task as difficulties associated with data collection and inference often result in inaccurate estimates. Two main methods for tree growth estimation are diameter tape measurements and increment cores. The former involves repeatedly measuring tree diameters with a cloth or metal tape whose scale has been adjusted to give diameter readings directly. This approach has the advantage that diameters can be measured rapidly. However, because of the substantial error involved during tape measurements, negative diameter increments are often observed. Alternatively, annual radius increment data can be obtained by taking tree cores and averaging repeated measurements of the ring widths. Acquiring and analyzing tree cores is a time-consuming process, and taking multiple cores may have adverse effects on tree health. Therefore, radius increment data are typically only available for a subset of trees within a stand. We offer a fusion of the data sources, which enables us to accommodate missingness and to borrow strength across individuals. It enables individual tree-level inference as well as average or stand level inference. Our model recognizes that tree growth in a given year depends upon tree size at the start of the year as well as levels of appropriate covariates operating in that year. We apply our modeling to a fairly large dataset taken from two forest stands at Coweeta Hydrologic Laboratory in the southern Appalachians collected from 1991 to 2011.

Keywords: continuous rank probability score; data fusion; Gaussian process; hierarchical Bayesian model; latent process; Markov chain Monte Carlo

1. INTRODUCTION

Tree growth is an important facet of forest dynamics and can inform about the health, productivity, and sustainability of a forest, as well as the spatial and temporal variability in growth rates. Dynamics that depend on a clear understanding of tree growth include species interactions (Swetnam and Lynch, 1993), carbon sequestration (Graumlich, 1991; DeLucia *et al.*, 1999; Caspersen *et al.*, 2000), population dynamics (Webster and Lorimer, 2005), and forest restoration (Pearson and Vitousek, 2001). However, tree growth estimation is a challenging task as difficulties associated with data collection and resultant inference often provide poor estimates. Forest mensuration and dendrochronology are two main foci within this body of research. The former incorporates quantitative measurements, such as diameter tape measurements, of trees within the forest stand to evaluate productivity and health (Husch *et al.*, 2002). Dendrochronology, or "tree-ring dating," on the other hand, uses increment cores to determine the date in which the rings were formed and thus the age of the tree (Schweingruber, 1988; Cook and Kairiukstis, 1990).

Diameter tape measurements and increment cores are both methods for estimating tree growth. Diameter tape measurements are obtained by repeatedly measuring the perimeter of the convex hull of the tree with a cloth or metal tape. The diameter is then estimated by dividing the perimeter by π (see Matérn (1956) for further discussion on this estimation). To expedite this process, measuring tapes are on the scale of the adjusted perimeter and give diameter readings directly. This approach has the advantage that diameters can be measured rapidly. Furthermore, it can be used for species that do not produce identifiable annual rings. Therefore, diameter measurements are usually available for trees in the entire mapped stand.

In order to obtain a confident estimate of the growth, there has to be sufficient time elapsed between observations, usually two or three years. As a result, annual growth at the individual level is not recorded and must be interpolated. In addition, because of the substantial error involved during tape measurements (Biondi, 1999; Gregoire *et al.*, 1990), negative diameter increments are often observed (Clark and Clark, 1999). A tree grows each year, so the observed declines in diameter should be viewed as measurement error and could be attributable to shrinkage and swelling according to unstable moisture storage or nongrowth-related change in bark thickness. Perhaps more consequential is the measurement error that results from field errors (e.g., inconsistent measuring height or the failure to keep the measuring tape on the proper plane). Previous methods for dealing with negative increments include adding a constant to each observation such that all become positive or

* *Correspondence to: E. M. Schliep, Department of Statistical Science, Duke University, Box 90351, Durham, NC 27708, U.S.A. E-mail: erin.schliep@duke.edu*

a *Department of Statistical Science, Duke University, Durham NC, U.S.A.*

b *comScore, Inc. Reston, VA, U.S.A.*

discarding the negative observations entirely. These approaches are unappealing as they introduce bias, and the resulting increment estimates would depend on the arbitrary method used (Clark and Clark, 1999). A more natural approach would be to specify observed growth through a measurement error model. That is, as a summation of true growth plus generic measurement error where true growth from year to year is nonnegative, the measurement error allows for observable negative increments.

An alternative to diameter tape measurements is increment core data, which record nonnegative annual growth directly. Increment core data introduce additional challenges and different measurement uncertainty. First, a core is ideally taken along the radius extending out from the pith of the tree; however, in practice, the core is taken where the field technician thinks the core might be with varying accuracy. Second, the pith is generally not in the centroid of the stem (Matérn, 1956). Modeling to attempt to remedy these inconsistencies is outside the scope of this work. Here, we assume the radius estimate from the increment core is half the diameter from the tape measurement. Annual radius increments are obtained by repeatedly measuring and averaging the width of rings on the core, which vary in identifiability across species. Conifers in temperate environments, for example, usually have readily identifiable rings, whereas many diffuse porous hardwoods often have missing rings. In addition, it is time-consuming to obtain and analyze tree cores, and taking multiple cores may have negative effects on tree health. Coring can also induce a wounding response that modifies growth in the vicinity of the core, which can have impacts on subsequent diameter tape measurements (Norton, 1998). Therefore, radius increment data are typically only available for a subset of trees within a stand.

In a forest stand, both sampling effort and data collection at the tree level can be irregular. The available individual level data vary in terms of when the tree is tape measured and if/when an increment core was taken. Some trees have few diameter tape measurements and no increment cores. In such cases, it is advantageous to borrow strength from other observed trees when making inference, while taking into account the errors associated with each type of measurement.

The literature contains many methodologies for modeling tree-level growth within a forest. Regression methods have been used to approximate mean growth rate for a population (Condit *et al.*, 1993; Terborgh *et al.*, 1997; Baker, 2003). However, they do not borrow strength from the complete dataset nor do they estimate tree-to-tree differences and the variability associated with the population heterogeneity. The book by Weiskittel *et al.* (2011) outlines two types of tree-level growth models: tree distance dependent and tree distance independent. Distance-dependent models are developed under the assumption that the spatial arrangement of trees in a stand can greatly inform about competition between trees. Tree-independent models, on the other hand, are computationally easier and benefit from both high precision and resolution.

In comparison, the Bayesian state space model for growth (Carlin *et al.*, 1992; Calder *et al.*, 2003; Clark *et al.*, 2007) emerges as a more satisfying model because it incorporates spatial dependence and exploits benefits from both radius increment and diameter census data. Weather data can also be considered and may provide valuable information as indicated by previous research on forest response to climate change (Bréda *et al.*, 2006; Allen *et al.*, 2010; Vilà-Cabrera *et al.*, 2011).

We advance this work in several ways. We present a method for tree growth estimation when the foregoing two types of data are available, exhibiting the irregularities mentioned earlier. We offer a fusion of the data sources, which enables us to accommodate missingness and to borrow strength across individuals. It facilitates individual tree-level inference as well as average or stand level inference. Specifically, a Bayesian hierarchical model is developed to infer true annual diameter growth at the tree level by fusing radius increment data and diameter census data. We explain growth using current size (implicit detrending) as well as appropriate weather data. We also incorporate spatial structure, anticipating similar relative growth for proximate trees, adjusted for the covariates. This also enables fusion even if the two data sources measure disjoint collections of trees. The spatial fusion model and three associated submodels are applied to a fairly large dataset taken from two forest stands at Coweeta Hydrologic Laboratory collected from 1991 to 2011. Model comparison raises an interesting issue when data sources vary between models. That is, when two datasets supply growth information in different forms, how do we demonstrate that the fusion model predicts growth better than say a model using solely tape measurement diameter data? We offer a natural way to address this question and compare the proposed models.

The format of the paper is as follows. In Section 2, we describe the Coweeta Hydrological Laboratory data. Section 3 presents our ensemble of models and some detail on the associated model fitting. Section 4 presents the analysis of the data under these models and the results of the model comparison. We conclude in Section 5 with a summary and indications of future work.

2. THE DATA

2.1. Tape-measured diameter and increment core data

Diameter measurement data were obtained from two mapped stands at Coweeta Hydrologic Laboratory in the southern Appalachians. Stand 1 is an oak-pine forest system, and stand 2 is a cove hardwood forest. The stands were established in 1991 for the purpose of studying forest dynamics (Clark *et al.*, 1998; Beckage *et al.*, 2000). The measurements are made at breast height, which is marked by a tree tag with an identifying tree number (Clark *et al.*, 2007). Diameter censuses were conducted at intervals of 1–4 years starting in 1993. Annually, some trees died and were removed, while new trees were planted and added, resulting in different numbers of trees measured in each census.

Increment cores at breast height were also obtained on a subset of trees (roughly 20%) within each of the two stands starting in 1998. Additional cores were collected in the years 2001, 2006, and 2009. Some trees were sampled in multiple years resulting in more than one set of increments observed for the tree. For example, a tree observed in 1998 and again in 2000 will have two increment core measurements for each year beginning with the year of the first ring through 1998 and then one increment core observation for the years 1999 to 2006. Note that the first ring is from the year that the tree reached breast height.

Illustratively, and in consultation with J. S. Clark, developer of the stands, the weather data we use to explain the between year variation in tree growth consist of annual precipitation, average summer (June–September) Palmer Drought Severity Index (PDSI), and average winter (January–March) temperature. These data are available for the years 1940–2013 and are stand specific.

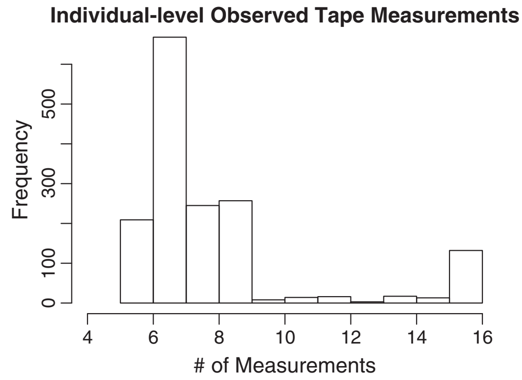

Figure 1. Histogram of the number of tape measurements made on each tree in the region

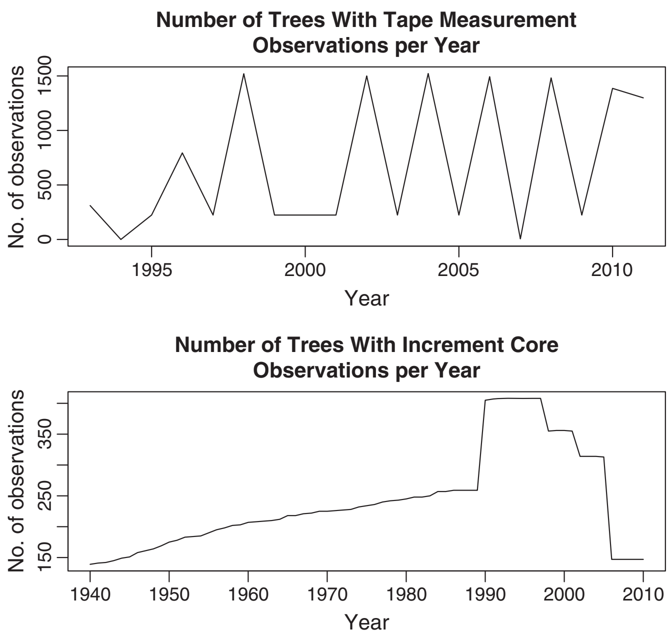

Figure 2. Number of diameter measurements and increment cores observed by year

2.2. Exploratory data analysis

We included all trees that had 5 or more diameter measurement observations from 1991 to 2011. Figure 1 shows a histogram of the number of diameter measurement cores observed per tree. Most trees have 5–7 diameter measurements, although some have as many as 15. The total number of distinct trees over the two stands in Coweeta Hydrologic Laboratory is 1583.

Increment cores were taken on 324 distinct trees, resulting in 1259 trees having only diameter measurements. The number of cores for a given tree ranged from 0 to 6. That is, 241 trees had one core, 76 had two cores, 6 had three cores, and 1 tree had five cores. Recall that an increment core provides an annual growth observation back to the year in which the tree reached breast height. Diameters were observed as early as 1993 for some trees, and many years are missing. For some trees, increment cores can be dated as far back as 1940. Figure 2 shows the number of diameter measurements and increment cores observed by year. Overall, the total number of diameter measurements is 13,105, and the total number of yearly increments observed is 17,108.

Figure 3 shows examples of two trees having both diameter measurements and increment cores. Diameter measurements often report negative growth, as shown in Figure 3(b). This tree also had two increment cores observed, although the second was missing before 1990.

Figure 4 shows the locations of the trees in stands 1 and 2 in the forest. Trees having only diameter measurements are indicated by circles, while those having both diameter measurements and increment cores are denoted by x's and are dispersed throughout each stand. These stands are each roughly 0.5 ha, and stand 1 is 200 m north of stand 2. Finally, Figure 5 shows the annual weather data to be used as covariates for the years 1940–2011 for stand 1. We see substantial annual variation, encouraging the hope that they can help to explain annual growth.

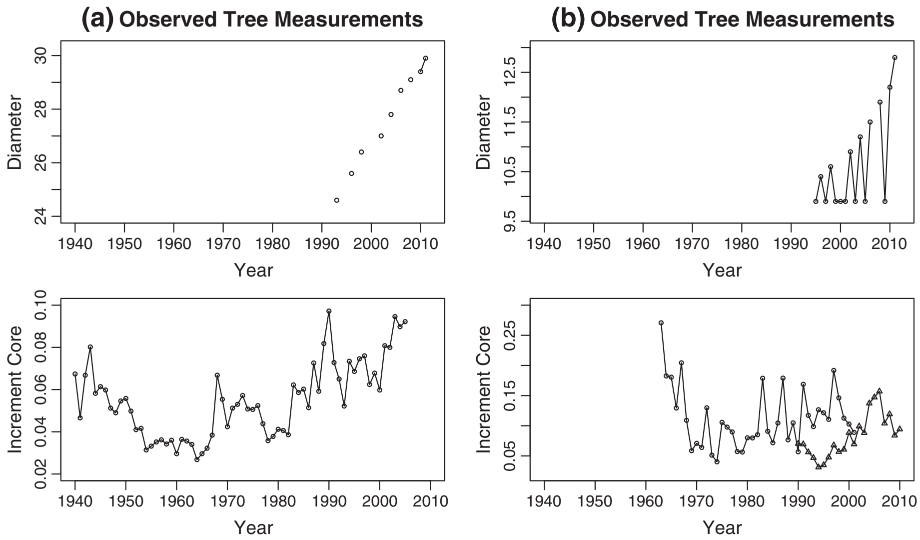

Figure 3. Tape measurement diameter (top) and increment cores (bottom) for two random trees, (a) left and (b) right. The second tree had two core observations, one taken in 2001 and another in 2009

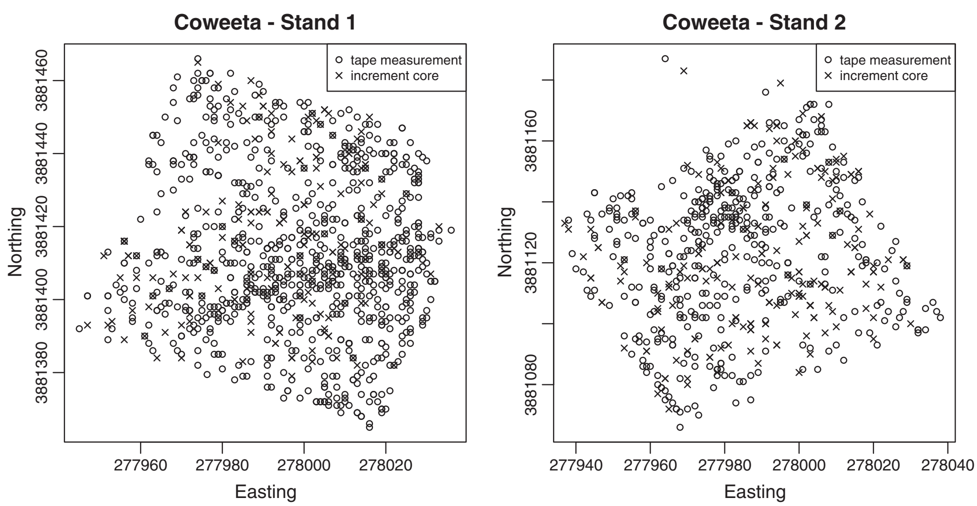

Figure 4. Stands 1 and 2 at Coweeta Hydrologic Laboratory. Easting and Northing coordinates given in Universal Transverse Mercator coordinates (UTMs)

3. MODELS

We consider both nonspatial and spatial model specifications, introducing the former in Section 3.1 and the latter in Section 3.2. Additionally, we analyze the diameter data separately and then introduce the fusion with the increment core data in order to assess the benefit of the additional data. Of course, either diameter census data or increment core data can be modeled separately to draw inference on tree growth. However, because the diameter data provide a complete census of the stands in our dataset, we chose it to provide the *baseline* relative to the fusion.

3.1. Nonspatial model specification

3.1.1. Diameter only models

For diameter census data, let $t = 0$ denote the year in which the first observation is available. Let $Y_{i,t}$ be the observed diameter and $\mu_{i,t}$ be the true diameter of tree i in year t. Because we are interested in individual growth, we set $\mu_{i,0} = Y_{i,0}$ and model $Y_{i,t}$, for t = 1, 2,... Let $\epsilon_{i,t}$ denote the measurement error of the diameter for tree i in year t. At the data level, the observed diameter of tree i in year t is the sum of its true diameter, $\mu_{i,t}$, and the measurement error $\epsilon_{i,t}$. That is,

$$Y_{i,t} = \mu_{i,t} + \epsilon_{i,t} \quad (1)$$

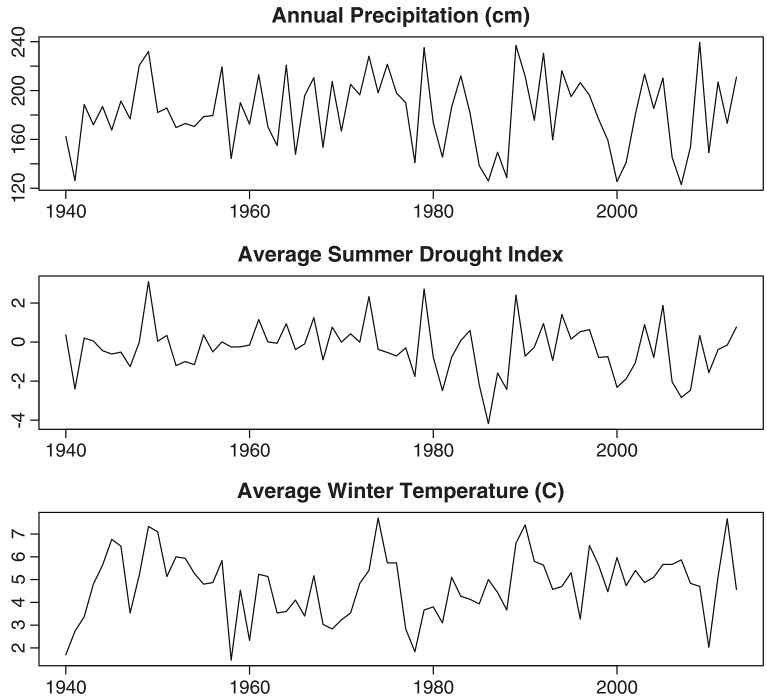

Figure 5. Annual precipitation, average summer Palmer Drought Severity Index, and average winter temperature for stand 1 from 1940 to 2011

The *true* diameter growth of tree i in year t, written as $\mu_{i,t} - \mu_{i,t-1}$, is assumed to be explained by the size of the tree at the start of the year, $\mu_{i,t-1}$, a global growth rate, the weather in year t, and a tree-specific random effect. Therefore, diameter growth is written as

$$\mu_{i,t} - \mu_{i,t-1} = \mu_{i,t-1}\alpha \exp\left(\mathbf{X}'_{i,t}\boldsymbol{\beta} + \omega_i\right) \tag{2}$$

where α is the *global* scale growth rate relative to current size, $\mathbf{X}_{i,t}$ denotes a vector of weather data for tree i and time t, $\boldsymbol{\beta}$ denotes a vector of coefficients, and ω_i is a tree-level random effect. Specifically, $\mathbf{X}_{i,t}$ consists of the annual precipitation, the average summer (June–September) PDSI, and the average winter (January–March) temperature and $\boldsymbol{\beta} = (\beta_1, \beta_2, \beta_3)'$. These values are plot specific. Here, α is intrinsically positive, and ω_i is used to capture the variation in response to weather at the tree level. We allow each tree to respond to the weather differently and, hence, grow at a different rate under the same weather conditions. One could also imagine that ω_i serves as a surrogate for unobservable covariates associated with the tree at location i. We assume $\omega_i \overset{i.i.d.}{\sim} N(0, \tau^2)$.

Under this model specification, true tree growth is nonnegative. The covariates and random effect provide a time and tree-specific scaling of growth rate. Because $\exp(\mathbf{X}'_{i,t}\boldsymbol{\beta} + \omega_i)$ can be either > 1 or < 1, it reflects a *relative risk*. Returning to (1), we assume $\epsilon_{i,t} \overset{i.i.d.}{\sim} N(0, \sigma^2)$ and note that future work will explore heterogeneous variance specifications. We adopt customary weak priors, that is, $\boldsymbol{\beta} \sim \mathrm{N}_3(\mathbf{0}, 10^4\mathbf{I})$, $\sigma^2 \sim \mathrm{IG}(2, 2)$, $\tau^2 \sim \mathrm{IG}(2, 2)$, and $\alpha \sim \mathrm{IG}(0.01, 1)$. Finally, the recursion in $\mu_{i,t}$ enables us to rewrite the model as

$$Y_{i,t} | \boldsymbol{\beta}, \omega_i \sim \mathrm{N}\left(\mu_{i,0} \prod_{k=1}^{t} \left(1 + \alpha \exp\left(\mathbf{X}'_{i,k}\boldsymbol{\beta} + \omega_i\right)\right), \sigma^2\right) \tag{3}$$

noting that only the observed $Y_{i,t}$'s appear in the likelihood associated with (3).

3.1.2. *The fusion model*

We extend the model to incorporate both diameter census data and radius increment data. This can be achieved by supplying an additional model for the radius increment data and assuming both sources of data share the same model for growth. Unlike the diameter census data, which gives the tree diameter measurements in certain years, the radius increment data reports the annual increase of tree radius from measuring the ring widths on the increment cores. As noted in Section 1, we make the simplifying assumption that the radius increment is half of the diameter increment and thus model the mean radius increment as $\frac{1}{2}(\mu_{it} - \mu_{i,t-1})$. Letting $Z_{i,t,j}$ denote the jth core measurement for tree i and year t, we define the model as

$$Z_{i,t,j} \sim \mathrm{N}\left(\frac{1}{2}\mu_{i,t-1}\alpha \exp\left(\mathbf{X}'_{i,t}\boldsymbol{\beta} + \omega_i\right), \gamma^2\right) \tag{4}$$

where $j = 1, \ldots, J_i$ and J_i is the number of cores for tree i. The measurement error variance for the radius increments is γ^2. Here, we assume conditionally independent measurement errors over j, resulting in marginally dependent errors due to the common ω_i. Again, the recursion provides the mean in the form

$$\frac{1}{2}\left(\alpha\exp\left(\mathbf{X}'_{i,t}\boldsymbol{\beta} + \omega_i\right)\right)\mu_{i,0}\left(\prod_{k=1}^{t-1}\left(1 + \alpha\exp\left(\mathbf{X}'_{i,k}\boldsymbol{\beta} + \omega_i\right)\right)\right)$$

The same prior distributions are employed as in the previous section, adding a weak inverse Gamma, IG(2, 2) prior for γ^2.

3.1.3. *Model fitting using Markov chain Monte Carlo*

The likelihood for the fusion model is proportional to the product of the likelihood of all observations in both the diameter census data and radius increment data, that is,

$$\begin{aligned} L(\boldsymbol{\beta}, \sigma^2, \gamma^2, \tau^2; \boldsymbol{X}, \boldsymbol{Y}, \boldsymbol{Z}) \propto & \prod_{i=1}^{n_y}\prod_{t=1}^{T_i} \mathrm{N}\left(Y_{i,t}; \left(\mu_{i,0}\prod_{k=1}^{t}(1 + \alpha\exp(\boldsymbol{X}'_{i,k}\boldsymbol{\beta} + \omega_i))\right), \sigma^2\right) \\ & \times \prod_{i=1}^{n_z}\prod_{j=1}^{J_i}\prod_{t=1}^{T_{i,j}} \mathrm{N}\left(Z_{i,t,j}; \frac{1}{2}(\alpha\exp(\mathbf{X}'_{i,t}\boldsymbol{\beta} + \omega_i))\Pi_{k=1}^{t-1}(1 + \alpha\exp(\mathbf{X}'_{i,k}\boldsymbol{\beta} + \omega_i)), \gamma^2\right) \\ & \times \prod_{i=1}^{n_y} \mathrm{N}\left(\omega_i; 0, \tau^2\right) \end{aligned} \tag{5}$$

We use Markov chain Monte Carlo to draw inference on our model parameters. Our Markov chain Monte Carlo algorithm is a Metropolis–Hastings within Gibbs sampler because the variance parameters, σ^2, γ^2, and τ^2, have conjugate full conditional posterior distributions, while ω_i, and $\boldsymbol{\beta}$, and α require Metropolis–Hastings steps. Estimates of the true diameter for each tree in each year are obtained using the posterior predictive distributions enabling the estimation of the true diameter of trees in unobserved years.

3.2. Spatial model specification

Although the two forest stands are only 200 m apart, we have elected to fit each one with a separate spatial model. We think the notion of spatial range emerges more clearly without having an imposed gap in the region, which would arise under a single model. This seems even more appropriate given that the maximum inter-tree distance within a stand is only 121 m. The only change made from the previous modeling is with regard to the tree-level random effects, where, now, the random effects on each stand are modeled as a realization of a Gaussian process (GP). Let $\boldsymbol{\omega}_k$ be a vector of the tree-specific random effects for trees on stand k for $k = 1, 2$. Then, independently for each k,

$$\boldsymbol{\omega}_k \sim GP(\mathbf{0}, \Sigma_k) \tag{6}$$

where $(\Sigma_k)_{ij} = \tau^2\rho(d_{ij}, \phi_k)$. Here, τ^2 is the spatial variance, and ρ is a valid correlation function with decay parameter ϕ_k. We adopt an exponential correlation function for ρ such that the correlation between locations i and j on stand k is a function of the distance, d_{ij}, between tree i and tree j and $\mathrm{corr}(\omega_i, \omega_j) = \exp(-d_{ij}/\phi_k)$.

The maximum distance between trees within a stand is 121 m. Uniform distributions are assigned to the decay parameters, ϕ_1 and ϕ_2, with lower and upper bounds of 0 and 30, respectively. Samples from the posterior for both ϕ_1 and ϕ_2 are obtained using a Metropolis–Hastings algorithm. As noted, the spatially correlated random effects replace the independent and identically distributed random effects in (2) under both the diameter only model and the data fusion model.

3.3. Model comparison approaches

We compare the diameter data only model and data fusion model with both the nonspatial and spatially correlated random effects. Altogether, the following four models are considered:

1. Diameter only, nonspatial model
2. Diameter only, spatial model
3. Fusion, nonspatial model
4. Fusion, spatial model.

Out-of-sample prediction is conducted on 500 trees selected at random. Each model is fitted using the remaining 1083 trees, of which 228 have one or more observed increment core. Of the 500 holdout trees, 96 have one or more increment core. Therefore, we have both diameter measurements and increment core measurements to assess out-of-sample prediction.

Because of the exponentiation of the random effect in the model as well as the recursion through time, the posterior predictive distribution of diameter can be highly skewed to the right. Therefore, we use the median of the posterior distribution for prediction and the median absolute prediction error (MAPE) to compare across models. We also compare the models using the continuous rank probability score (CRPS) (Gneiting and Raftery, 2007). The CRPS is attractive in that it compares an observed value with an entire predictive distribution. The more concentrated the distribution is around the observation, the smaller the CRPS. The MAPE and CRPS are computed separately for the diameter holdout data and for the increment core holdout data.

We conclude this section with an important point. Suppose validation for the diameter only model is performed using only out-of-sample diameter data, whereas validation for the fusion model is performed using both out-of-sample diameter and increment core data. It is evident that this confuses assessment of the performance of the latter relative to the former. When the additional data are not diameters, one should not expect the fusion model to validate better than the diameter only model for the holdout diameter data. That is, the fusion model helps to better learn about true growth but need not predict holdout diameters better.

The fusion model is expected to do well in predicting diameters and also in predicting increment cores. Arguably, the clearest way to reveal the benefit of the fusion model is to see how well the diameter only model predicts radius increments. There is a predictive distribution for radius increments under the diameter only model. It arises from the posterior samples of diameter pairs at consecutive time points. We present out-of-sample MAPE and CRPS for the diameter only models and the fusion models for both tape measurement diameter and increment core prediction. Note that because the diameter and increment core data are on different scales, we do not attempt to obtain an overall model performance measure. Rather, prediction and model comparison is performed for each data type separately.

4. DATA ANALYSIS

The models were fitted for 150,000 iterations where the first 100,000 iterations of the chain were discarded as burn-in. Figures 6 and 7 give the posterior prediction medians and 90% credible intervals for diameter measurements and increment cores, respectively, for an illustrative tree under each of the four models. Also shown are the observed diameter and increment core measurements in the plots, respectively. We

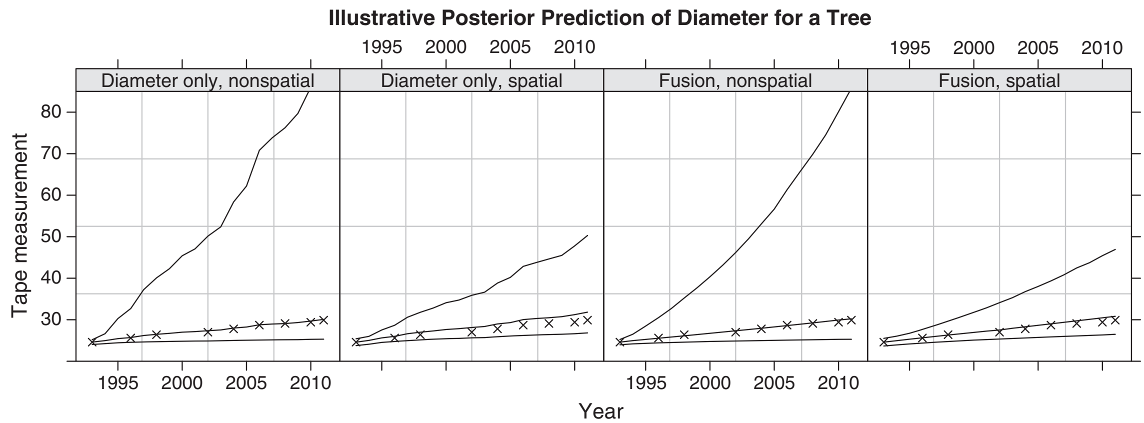

Figure 6. Medians and 90% credible intervals of the posterior predictive distributions of diameter for an individual tree under the four models. Also shown are the observed diameter measurements for the tree

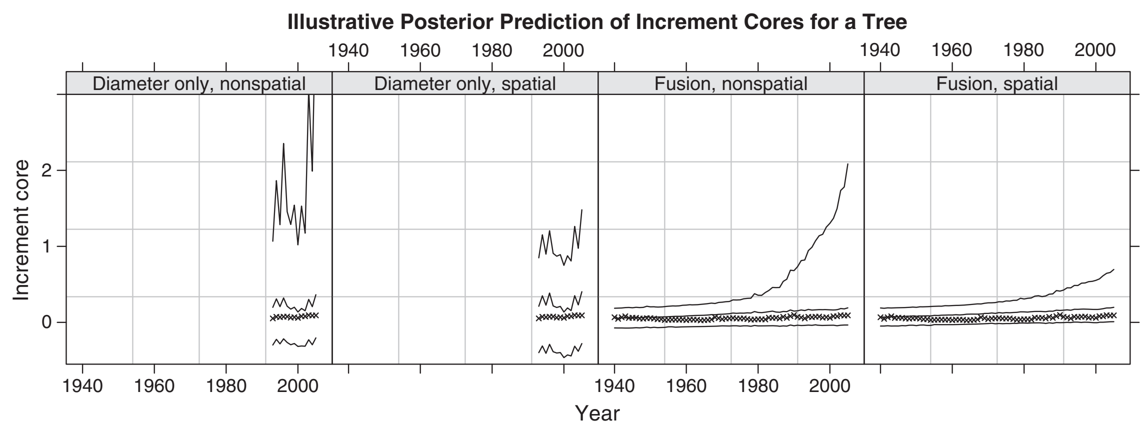

Figure 7. Medians and 90% credible intervals of the posterior predictive distributions of increment cores for an individual tree under the four models. Also shown are the observed increment cores for the tree

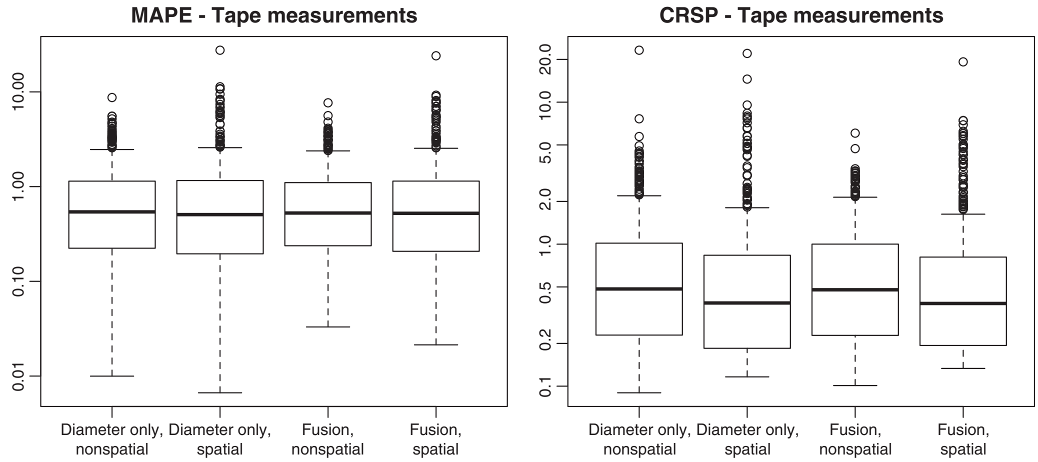

Figure 8. Boxplots of the out-of-sample median absolute prediction error (MAPE) and continuous rank probability score (CRPS) for tape measurement data for each tree for the four models

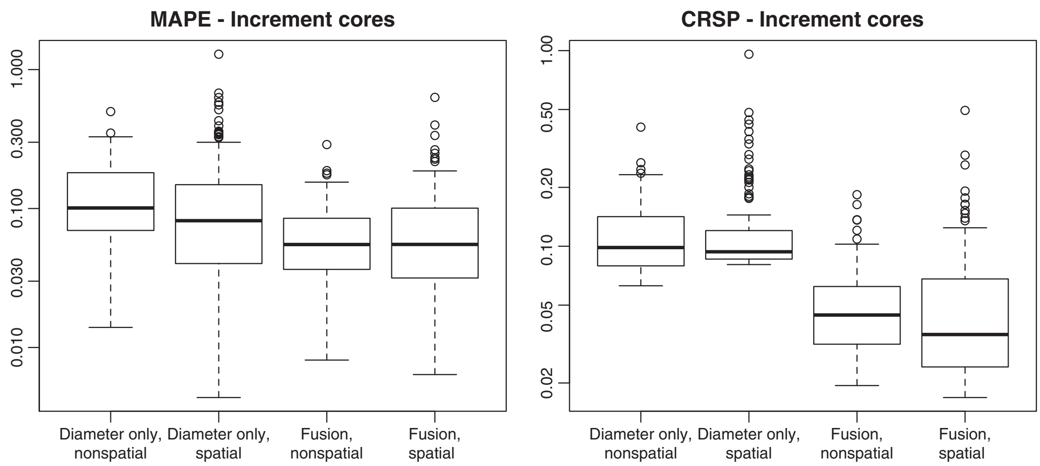

Figure 9. Boxplots of the out-of-sample median absolute prediction error (MAPE) and continuous rank probability score (CRPS) for increment core data for each tree for the four models

predict out-of-sample increment cores using the diameter only models for only the years 1993–2010 to avoid extrapolating outside the range of the tape measurement data observed. In general, the nonspatial models have wider credible intervals, in support of the spatial models. The spatial models are similar for predicting the illustrative tree's diameter. However, the diameter only spatial model has much wider credible intervals for the increment cores than the spatial fusion model.

Figure 8 gives boxplots of MAPE and CRPS for diameter measurements for each tree in the holdout set for the four models. The medians and quantiles of these prediction criteria are very similar across the models. Figure 9 gives the same boxplots for the out-of-sample increment cores for the four models. The fusion models show slight improvements over the diameter only models in terms of the absolute deviation. However, CRPS clearly indicates superior out-of-sample prediction of increment cores for the fusion models. Additionally, both MAPE and CPRS are slightly lower for the spatial fusion model than the nonspatial fusion model. To assess bias, we compute the proportion of overprediction for each model and data source. For the tape measurement data, the proportion of overprediction is between 0.55 and 0.57 for the four models. The proportion of overprediction for the increment cores is between 0.62 and 0.67, except for the nonspatial diameter only model, in which the proportion of overprediction is 0.78. This notable bias toward overprediction is the result of the noisy tape measurement data and the absence of the more precise increment core data.

Figure 10 shows MAPE and CRPS for out-of-sample prediction for the diameter data over all trees by year for each of the four models. MAPE is fairly similar across the four models. CRPS tends to slightly favor the spatial models over the nonspatial models. The spikes in each of the two plots in years 2003, 2005, and 2009 are years in which there were few diameter observations in the out-of-sample data. MAPE and CRPS for out-of-sample prediction for the increment core data over all trees by year are given in Figure 11. MAPE slightly favors the spatial fusion model over the nonspatial fusion model over all years. In some years, however, the diameter only models report slightly lower MAPE than the fusion models. CRPS greatly favors the fusion models over the diameter only models, and the spatial fusion model has the lowest CRPS for all years. The spikes seen in the last 5 years are again due to few trees in the out-of-sample data having observed cores in those years.

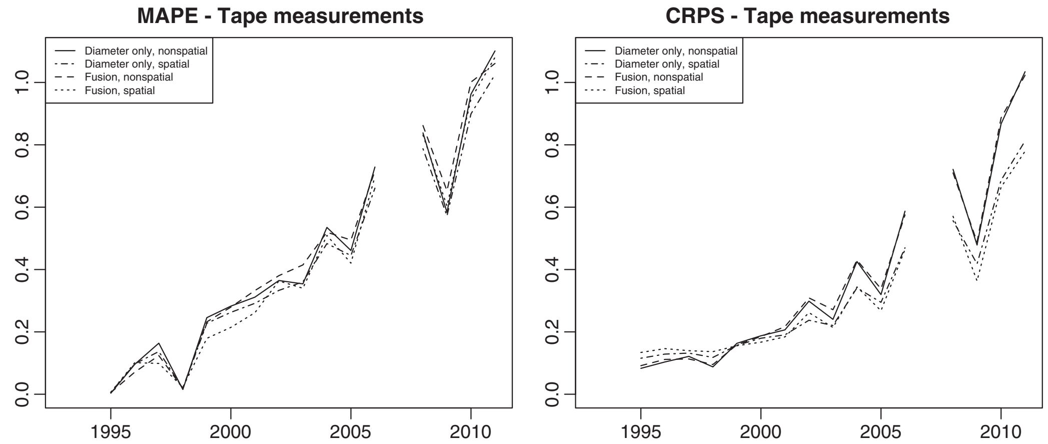

Figure 10. Median absolute prediction error (MAPE) and continuous rank probability score (CRPS) for tape measurement data by year for the four models

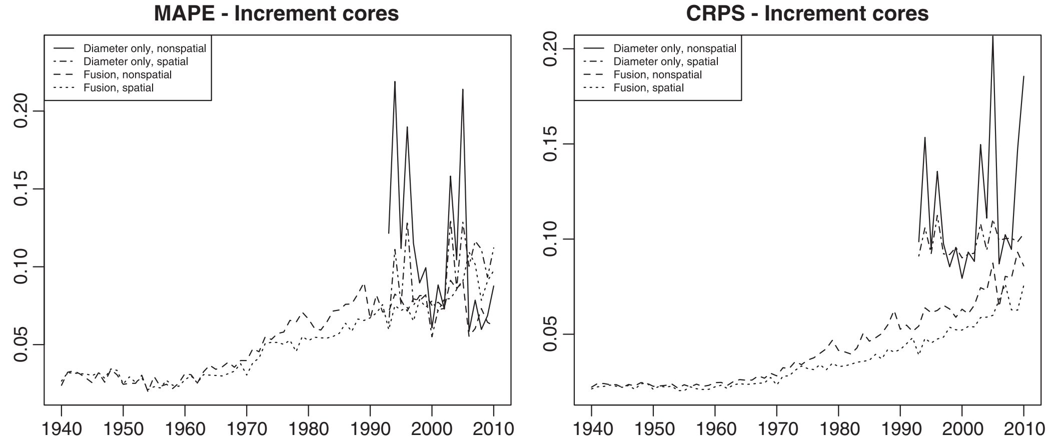

Figure 11. Median absolute prediction error (MAPE) and continuous rank probability score (CRPS) for increment core data by year for the four models

Table 1. Posterior median and 90% credible intervals for the variance parameters of the four models

	Parameter	Diameter only, nonspatial	Diameter only, spatial	Fusion, nonspatial	Fusion, spatial
τ^2	Spatial variance	1.39 (1.28, 1.50)	1.67 (1.37, 2.31)	1.23 (1.15, 1.33)	1.18 (1.03, 1.42)
$3\phi_1$	Effective range (stand 1)		23.93 (17.60, 36.99)		15.37 (11.00, 21.38)
$3\phi_2$	Effective range (stand 2)		8.39 (6.66, 11.97)		7.24 (5.98, 8.94)
σ^2	Tape measurement error	0.13 (0.12, 0.13)	0.24 (0.23, 0.26)	0.15 (0.15, 0.16)	0.33 (0.31, 0.34)
γ^2	Core measurement error			0.0058 (0.0057, 0.0060)	0.0049 (0.0048, 0.0051)

Table 1 gives posterior median and 90% credible intervals for the variance parameters of the four models. This includes the variance parameters of the tree-level random effects as well as the measurement error variances for the two data sources. Note that the variance of the random effects is smaller under the spatial models suggesting that the smoothness captured by spatially structured random effects is preferable to the independent effects under the nonspatial models. Further, there appears to be a trade-off between the spatial and nonspatial models in terms of the measurement error variances between the two data sources. The measurement error variance for the tape measurement data, σ^2, is larger in the spatial models than in the nonspatial models, while the measurement error for the increment core data, γ^2, is smaller in the spatial model than nonspatial model.

Posterior median and 90% credible intervals for the spatial fusion model parameters are given in Table 2. The coefficient parameters for annual precipitation and winter temperature behave as expected. The coefficient for annual precipitation is significant and indicates that

Table 2. Posterior median and 90% credible interval for the spatial fusion model parameters

	Parameter	Median	90% CI
β_1	Annual precipitation	0.0270	(0.0165, 0.0373)
β_2	Summer PDSI	−0.0025	(−0.0217, 0.0166)
β_3	Winter temperature	−0.0051	(−0.0186, 0.0081)
α	Global growth rate	0.0094	(0.0091, 0.0099)
τ^2	Spatial variance	1.18	(1.03, 1.42)
$3\phi_1$	Effective range (stand 1)	15.37	(11.00, 21.38)
$3\phi_2$	Effective range (stand 2)	7.24	(5.98, 8.94)
σ^2	Tape measurement error	0.33	(0.31, 0.34)
γ^2	Core measurement error	0.0049	(0.0048, 0.0051)

annual tree growth tends to increase with an increase in annual precipitation. Annual tree growth tends to decrease with increased dryness, that is, larger summer PDSI. Lastly, higher winter temperatures tend to decrease annual tree growth. This may be related to higher respiration losses outside the growing season, which has been shown for loblolly pine stands in North Carolina (Sampson *et al.*, 2006). Also, the posterior estimate of the variance for tape measurement is 0.33 cm^2 and for increment cores is 0.0049 cm^2, a reflection of the fact that the increment core data are much more precise than the diameter data. The effective range is the distance beyond which the correlation between two observations is less than 0.05. This indicates that the range of spatial correlation is further in stand 1 (roughly 15 m) than in stand 2 (roughly 7 m).

5. SUMMARY AND FUTURE WORK

We have dealt with the challenge of learning about individual tree growth in a somewhat novel fusion setting where we have a noisy but full inventory data source of diameter measurements along with a smaller but historically longer and more precise source of increment core data for a forest stand. We have implemented a hierarchical model with spatial dependence through a latent true growth specification. This specification provides a growth model that reflects current size of individuals along with explanatory weather variables and tree-level spatial random effects. With regard to predicting growth, this model outperforms submodels, which omit either the data fusion or the spatial aspect. We have also clarified why, for predicting diameters, the diameter data only model and the fusion model are essentially equivalent. Primarily, the two data sources inform differently about the *true* individual growth process. By contrast, more familiar data fusion models typically combine monitored data with computer model output for the *same* variable. However, with regard to the growth process, we believe the fused, spatial model is more appealing mechanistically and behaviorally.

The novelty in the model present here takes us beyond the customary tree growth models in the literature, such as those cited in Section 1. The latent growth model imposes nonnegative growth and is informed by two sources of data. Additionally, time and location varying weather information is employed to help explain the annual variation in growth rates. Lastly, we incorporate a global scale growth rate with individual random effects. These random effects, or rather, individual random adjustments to the global scale growth rate, borrow strength across individuals to learn about these adjustment. An attractive feature of working with the spatial model is that there is no requirement that the data contain trees with both tape measurement and increment core observations. With spatially structured random effects, we can still implement data fusion and borrow strength across the two datasets to better learn about individual tree performance.

There are several simplifying assumptions in the proposed model, and their limitations will guide future work. First, both the model for diameter tape measurements and the model for increment core measurements need to be refined to better reflect the way in which the measurements are actually obtained and hence the associated bias and noise they introduce. That is, we need to consider richer noise structure than simple normal errors. Another extension to the model is to introduce suitable heterogeneity in the uncertainty associated with the noise to potentially reflect space, time, and current size. In order to compare growth and the response to weather data at the species level, we need to also incorporate species information into the model. Lastly, exploring growth for a broader geographic region will enable investigation on a larger spatial scale and incorporation of a richer palette of weather conditions.

Acknowledgements

The authors thank Jim Clark for providing the forest data and for valuable conversations. The work of the first and third authors was supported in part by NSF DEB 0842465.

REFERENCES

Allen CD, Macalady AK, Chenchouni H, Bachelet D, McDowell N, Vennetier M, Kitzberger T, Rigling A, Breshears DD, Hogg EH, Gonzalez P, Fensham R, Zhang Z, Castro J, Demidova N, Lim J, Allard G, Running SW, Semerci A, Cobb N. 2010. A global overview of drought and heat-induced tree mortality reveals emerging climate change risks for forests. *Forest Ecology and Management* **259**(4):660–684.

Baker PJ. 2003. Tree age estimation for the tropics: a test from the southern Appalachians. *Ecological Applications* **13**(6):1718–1732.

Beckage B, Clark JS, Clinton BD, Haines B L. 2000. A long-term study of tree seedling recruitment in southern Appalachian forests: the effects of canopy gaps and shrub understories. *Canadian Journal of Forest Research* **30**(10):1617–1631.

Biondi F. 1999. Comparing tree-ring chronologies and repeated timber inventories as forest monitoring tools. *Ecological Applications* **9**(1):216–227.

Bréda N, Huc R, Granier A, Dreyer E. 2006. Temperate forest trees and stands under severe drought: a review of ecophysiological responses, adaptation processes and long-term consequences. *Annals of Forest Science* **63**(6):625–644.

Calder C, Lavine M, Müller P, Clark JS. 2003. Incorporating multiple sources of stochasticity into dynamic population models. *Ecology* **84**(6):1395–1402.

Carlin BP, Polson NG, Stoffer DS. 1992. A Monte Carlo approach to nonnormal and nonlinear state-space modeling. *Journal of the American Statistical Association* **87**(418):493–500.

Caspersen JP, Pacala SW, Jenkins JC, Hurtt GC, Moorcroft PR, Birdsey RA. 2000. Contributions of land-use history to carbon accumulation in US forests. *Science* **290**(5494):1148–1151.

Clark DA, Clark DB. 1999. Assessing the growth of tropical rain forest trees: issues for forest modeling and management. *Ecological applications* **9**(3): 981–997.

Clark JS, Macklin E, Wood L. 1998. Stages and spatial scales of recruitment limitation in southern Appalachian forests. *Ecological Monographs* **68**(2): 213–235.

Clark JS, Wolosin M, Dietze M, Ibanez I, LaDeau S, Welsh M, Kloeppel B. 2007. Tree growth inference and prediction from diameter censuses and ring widths. *Ecological Applications* **17**(7):1942–1953.

Condit R, Hubbell SP, Foster RB. 1993. Identifying fast-growing native trees from the Neotropics using data from a large, permanent census plot. *Forest Ecology and Management* **62**(1):123–143.

Cook ER, Kairiukstis LA. 1990. *Methods of dendrochronology: applications in the environmental sciences*. Springer: Dordrecht, Netherlands.

DeLucia EH, Hamilton JG, Naidu SL, Thomas RB, Andrews JA, Finzi A, Lavine M, Matamala R, Mohan JE, Hendrey GR, Schlesinger WH. 1999. Net primary production of a forest ecosystem with experimental CO_2 enrichment. *Science* **284**(5417):1177–1179.

Gneiting T, Raftery AE. 2007. Strictly proper scoring rules, prediction, and estimation. *Journal of the American Statistical Association* **102**(477):359–378.

Graumlich LJ. 1991. Subalpine tree growth, climate, and increasing CO_2: an assessment of recent growth trends. *Ecology* **72**(1):1–11.

Gregoire T, Zedaker S, Nicholas N. 1990. Modeling relative error in stem basal area estimates. *Canadian Journal of Forest Research* **20**(5):496–502.

Husch B, Beers TW, Kershaw JA Jr. 2002. *Forest Mensuration*. John Wiley & Sons: Hoboken, New Jersey.

Matérn B. 1956. On the geometry of the cross-section of a stem. *Medd. Statens Skogsforskningsinst.*

Norton DA. 1998. *Impacts of Tree Coring on Indigenous Trees*. Department of Conservation: Wellington, New Zealand.

Pearson HL, Vitousek PM. 2001. Stand dynamics, nitrogen accumulation, and symbiotic nitrogen fixation in regenerating stands of Acacia koa. *Ecological Applications* **11**(5):1381–1394.

Sampson D, Waring R, Maier C, Gough C, Ducey M, Johnsen K. 2006. Fertilization effects on forest carbon storage and exchange, and net primary production: A new hybrid process model for stand management. *Forest Ecology and Management* **221**(1):91–109.

Schweingruber FH. 1988. *Tree Rings-Basics and Applications of Dendrochronology*. D. Reidel Publishing Company: Dordrecht, Netherlands.

Swetnam TW, Lynch AM. 1993. Multicentury, regional-scale patterns of western spruce budworm outbreaks. *Ecological monographs* **63**(4):399–424.

Terborgh J, Flores C, Mueller P, Davenport L. 1997. Estimating the ages of successional stands of tropical trees from growth increments. *Journal of Tropical Ecology* **13**(6):833–856.

Vilà-Cabrera A, Martínez-Vilalta J, Vayreda J, Retana J. 2011. Structural and climatic determinants of demographic rates of Scots pine forests across the Iberian Peninsula. *Ecological Applications* **21**(4):1162–1172.

Webster CR, Lorimer CG. 2005. Minimum opening sizes for canopy recruitment of midtolerant tree species: a retrospective approach. *Ecological applications* **15**(4):1245–1262.

Weiskittel AR, Hann DW, Kershaw JA Jr., Vanclay JK. 2011. *Forest Growth and Yield Modeling*. John Wiley & Sons: Oxford.

